High Intrachain Order Promotes Triplet Formation from Recombination of Long-Lived Polarons in Poly(3-hexylthiophene) J-Aggregate Nanofibers

Alan K. Thomas, José A. Garcia, Jordan Ulibarri-Sanchez, Jian Gao, and John K. Grey*

Department of Chemistry and Chemical Biology, University of New Mexico, MSC03 2060, Albuquerque, New Mexico 87131, United States

ABSTRACT Photoluminescence (PL) of single poly(3-hexylthiophene) (P3HT) J-aggregate nanofibers (NFs) exhibits strong quenching under intensity-modulated pulsed excitation. Initial PL intensities (I_0) decay to steady-state levels (I_{SS}) typically within ~1−10 μs, and large quenching depths (I_0/I_{SS} >2) are observed for ~70% of these NFs. Similar studies of polymorphic, H-aggregate type P3HT NFs show much smaller PL quenching depths ($I_0/I_{SS} \leq 1.2$). P3HT chains in J-type NF π-stacks possess high intrachain order, which has been shown previously to promote the formation of long-lived, delocalized polarons. We propose that these species recombine nongeminately to triplets on time scales of >1 ns. The identity of triplets as the dominant PL quenchers was confirmed by subjecting NFs to oxygen, resulting in an instantaneous loss of triplet PL quenching (I_0/I_{SS} ~1). The lower intrachain order in H-type NFs, similar to P3HT thin-film aggregates, localizes excitons and polarons, leading to efficient geminate recombination that suppresses triplet formation at longer time scales. Our results demonstrate the promise of self-assembly strategies to control intrachain ordering within multichromophoric polymeric aggregate assemblies to tune exciton coupling and interconversion processes between different spin states.

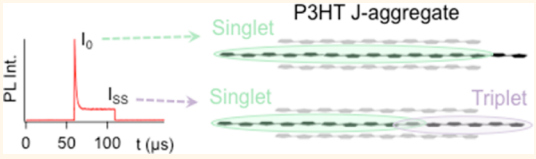

KEYWORDS: P3HT nanofibers · J-aggregate · triplet quenching · intrachain order · polaron recombination

Understanding the influence of conformation and packing on the electronic properties of conjugated polymers remains a long-standing challenge to optimize the performance of these materials for optoelectronic applications. In particular, the efficacies of energy and charge transfer along or through polymer chains as well as interactions and interconversion between electrically neutral exciton and charged polaron species are intimately dependent on the polymer structural attributes, which are usually difficult to control using conventional material processing techniques.[1,2] However, the tendency of some polymers to assemble into ordered, π-stacked aggregates can lead to efficient multidimensional (*i.e.*, intra- and interchain) charge and energy transport, which offer researchers greater opportunities to tune material functionality and improve performance.[3,4]

P3HT is perhaps the most recognized conjugated polymer system capable of forming extended aggregates, which has made it a benchmark material in solar cell and field-effect transistor applications. Following initial reports of efficient multidimensional charge and energy transfer in P3HT aggregates by Sirringhaus *et al.* and Osterbacka *et al.*, respectively, numerous studies have sought to further exploit aggregates to understand and improve device performance figures of merit. The development of the weakly coupled HJ aggregate exciton model by Spano and co-workers has proven a powerful tool in these efforts, which relates microscopic structure and ordering information to exciton coupling characteristics and strength from one-photon optical spectra.[5] This model has been used extensively in the study of P3HT aggregate optical and electronic properties and their dependence on intrachain (*i.e.*, monomer coplanarity) and interchain (*i.e.*, packing) order. Exciton coupling can be determined using the HJ aggregate

* Address correspondence to jkgrey@unm.edu.

Received for review July 20, 2014 and accepted October 2, 2014.

Published online October 06, 2014
10.1021/nn5040026

model by comparing the one-photon absorption strength of the pure electronic origin transition (0−0) to the first vibronic sideband (0−1).[5] 0−0/0−1 values of <1 are found for H-aggregate exciton coupling (*i.e.*, face-to-face dipole coupling), entailing greater interchain exciton character in the P3HT π-stack.[6] These excitons are most commonly observed in thin-film P3HT aggregates with low intrachain order arising from polydispersity-induced stacking faults and disorder.[7] On the other hand, 0−0/0−1 ratios of >1 have only recently been reported in P3HT aggregates, indicating high intrachain order that strongly attenuates interchain coupling (*e.g.*, $\ll k_BT$) due to extended intrachain exciton delocalization.[8] This is the J-aggregate coupling limit (*i.e.*, head-to-tail coupling) that arises only in situations when molecular weight fractionation occurs during the aggregate assembly leading to very few stacking faults. Because conventional processing methods of P3HT functional forms (*i.e.*, thin films) typically do not promote fractionation, this mode of exciton coupling is very rare in P3HT systems.[9] Our group has recently demonstrated that solution-based self-assembly of P3HT aggregate nanofibers (NFs, also known as nanofibrils or nanoribbons) can be used to select H−J exciton couplings through effective control of aggregate order and sizes as well as the boundaries between aggregated and amorphous domains. Importantly, the latter has been proposed to facilitate conversion of neutral excitons into free charge carriers (polarons), which makes the understanding and control of these features vital for further maximizing material performance.[10] This intrinsic charge generation mechanism has been demonstrated in P3HT thin films and has since generated interest in further understanding the structure−function relationships of this charge generation process.[11,12] Autoionization may also occur in single P3HT chains (typically within aggregates) either by hot exciton dissociation or delocalization-induced polaron pair formation.[13,14] In addition to forming charged species, long-lived triplet states may emerge and, together with polarons, interact with singlets generated on nearby chromophores *via* intra- or interchain mechanisms.[15] These interactions are mediated primarily by the polymer structural characteristics, but intrinsic nano- to micrometer scale morphological features tend to obscure specific molecular-level structural and conformational factors regulating triplet generation mechanisms and interactions.

Here, we study chain conformation- and packing-dependent exciton interconversion, interactions, and dynamics in P3HT aggregates by self-assembling two limiting NF structures with well-defined packing and ordering characteristics. Single NF photoluminescence (PL) modulation spectroscopy and imaging techniques are used that have already seen extensive use as probes for understanding the roles of conformation and packing on photophysical outcomes in conjugated polymers.[16−22] Exciton−polaron interactions[23−25] and singlet−triplet interactions[24,26,27] can also be interrogated on sub-100 nm size scales, and we now extend these studies to single P3HT NF structures by measuring PL quenching dynamics on ∼100 ns to 1 ms time scales. By carefully controlling the kinetics of nanofiber formation (*i.e.*, solvent−solute interactions), the intra- and interchain order and, hence, exciton coupling within aggregates can be tuned, thus affording more accurate structure−function information.[8,9] To this end, two types of P3HT NFs are studied that represent the limits of excitonic degrees of freedom in P3HT aggregates, namely, (i) highly ordered, crystalline J-aggregates and (ii) less ordered, polymorphic H-aggregates.[8,28]

Despite that the HJ aggregate model was originally developed considering neutral and optically accessible singlet excitons, its underpinnings can be extended to understand exciton−polaron interactions and interconversion processes outlined above. Specifically, intra- and interchain (packing) order and coupling inferred from singlet-exciton optical transition line shapes can teach us how these structural factors influence the branching ratios of S = 1/2 polaron and S = 1 triplet formation mechanisms and their interaction with singlets over a broad range of time scales.[20,23,29,30] In particular, the high sensitivity of P3HT NF aggregate singlet-chromophore exciton coupling makes PL probes very attractive for elucidating the dependence of exciton−polaron and singlet−triplet interactions on chain-ordering characteristics, which is exceedingly difficult in thin films due to inhomogeneity effects.[22,24] We demonstrate efficient quenching of J-aggregate NF PL intensities on microsecond time scales from triplet states generated primarily from nongeminate recombination of long-lived, intrachain-delocalized polarons generated on earlier time scales from autoionization of singlet excitons. This mechanism of triplet formation is not effective in conventional thin-film aggregates and less ordered H-type NF structures, because their lower intrachain order instead localizes excitons or polarons, which promotes faster relaxation, trapping, and geminate recombination processes.

RESULTS AND DISCUSSION

P3HT NFs are prepared and characterized using methods published earlier.[8,9] TEM images of H- and J-type NFs are shown in Figure 1a,b, respectively. H-type NFs are typically ∼15−20 nm wide and have a rope-like, segmented appearance that stems from their rapid formation kinetics in anisole. J-type NF widths, on the other hand, are ∼30−40 nm and have a more diffuse appearance reducing contrast in their TEM images, owing to slow self-assembly over several days in toluene. These conditions promote molecular weight fractionation, resulting in aggregates with very

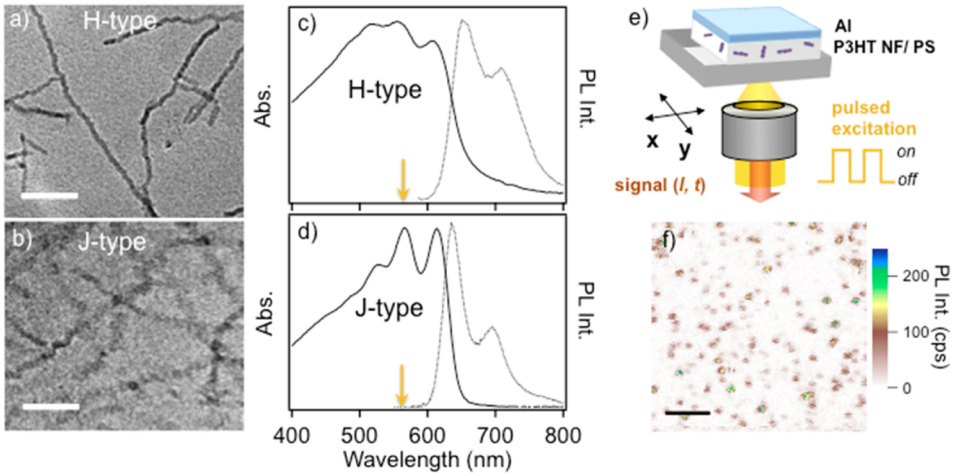

Figure 1. TEM images of H- (a) and J-type (b) P3HT NFs (scale bar = 200 nm). Optical absorption and PL spectra of H- (c) and J-type (d) P3HT NF dispersions. Arrows indicate excitation wavelengths used to excite PL in single NFs. (e) Scheme of excitation intensity modulated single-particle PL imaging and spectroscopy on P3HT NFs dispersed in polystyrene (PS) and sealed with an aluminum overcoating. (f) Representative PL image of single NFs dispersed within the PS host matrix. (scale bar = 5 μm).

few stacking faults. This effect does not occur in H-type NFs assembled in anisole and instead leads to polymorphic structures with poorer aggregate quality. Consequently, exciton coupling and intrachain ordering of P3HT chains comprising these NFs are distinctly different and can be assessed from optical absorption and PL spectra (Figure 1c,d) using the HJ aggregate model. J-type NFs possess high intrachain order that attenuates interchain coupling[31] due to the delocalized nature of singlet excitons. Recent time-resolved PL polarization anisotropy measurements also revealed that J-type excitons remain intrachain in nature throughout their entire lifetime.[32,33] H-type NF excitons are localized from disorder effects resulting in lower intrachain order and larger interchain coupling with adjacent chains in the aggregate π-stack.

Figure 1e highlights the experimental approach used in this study, where NFs are dispersed in an inert host matrix and interrogated using single-nanoparticle PL spectroscopy. The PL of individual NFs is excited using a sequence of laser pulses of varying intensities spanning the microsecond time scale regime. Samples are coated with aluminum to prevent unwanted photodegradation, and a typical PL image of well-dispersed NFs is shown in Figure 1f. Figure 2a displays a representative excitation intensity-modulated pulse sequence (I_{exc}) used to pump P3HT NF PL generated by shaping a CW laser with an acoustic optical modulator controlled by a function generator. Average excitation powers used were ~50 nW, corresponding to peak intensities of approximately 20 W/cm^2 (I), 95 W/cm^2 (II), 220 W/cm^2 (III), and 370 W/cm^2 (IV), and pulse cycle periods ranged from 500 μs up to 5 ms. Figure 2b,c show representative excitation intensity-dependent PL transients from H- and J-type P3HT NFs, respectively, recorded by synchronously averaging many pulse cycles

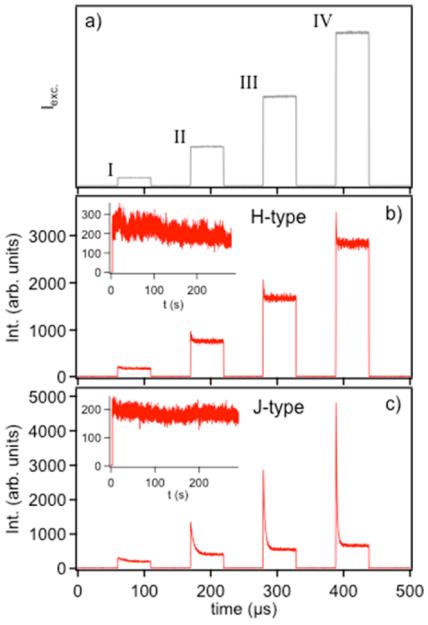

Figure 2. (a) Typical laser pulse excitation profile generated from scattered excitation light. See text for characteristic peak intensities for each pulse. Excitation intensity dependent transients were recorded using a multichannel analyzer (MCA) that synchronously averaged over many excitation cycles. (b, c) Representative transients of H-type and J-type P3HT NFs from over 100 individual particles. Insets show corresponding PL transients averaged over longer times (~1−10 ms) with a multichannel scaler. These longer time transients were used to assess the NF photostability characteristics over the course of the experiment.

using a multichannel analyzer (MCA). Once the laser turns on, the singlet-exciton PL intensity rises to its maximum (I_0) within the instrument-limited time resolution (~100 ns) usually followed by decay to a steady-state level (I_{SS}) at later times. Quenching dynamics time scales are similar between NF types, showing PL modulation, but quenching depths (I_0/I_{SS}), however,

are markedly different depending on the packing and intrachain order of chains within the NF aggregates. Excitation intensity-dependent transients were measured from many NF particles for each type (>100), including different batches, that show similar behavior as reported in Figure 2b,c. Polymorphic H-type NFs show relatively small average quenching depths ($I_0/I_{SS} \leq 1.2$, Figure 2b) for particles displaying any discernible quenching (~30%) whereas the majority of particles studied (62%) displayed no PL quenching. Conversely, J-type NFs exhibit much larger quenching depths ($I_0/I_{SS} \geq 2$) for ~70% of all particles studied, and PL modulation characteristics were independent of particle size (brightness, Figure 2c) as well as the overall excitation cycle frequency (see Supporting Information). A small fraction (7%) of all H-type NFs studied did show larger PL quenching depths, suggesting some of these structures are more J-like in nature. In a previous study of H-type NFs fabricated in anisole, PL excitation spectroscopy revealed that line shapes are dominated by minority, lower energy emitters populated by energy transfer from nearby higher energy chromophores.[34] Upon dispersing NFs in inert hosts, fragmentation occurs to varying degrees, meaning that energy transfer pathways are broken, and we propose the small fraction of H-type NFs displaying large PL quenching depths reflect these minority emissive traps. In a similar vein, approximately 20% of J-type NFs showed lower PL quenching depths ($I_0/I_{SS} < 1.5$) that were mostly smaller (*i.e.*, less intense) particles. For comparison, the same experiment was performed on regioregular P3HT thin films and P3HT nanoparticles prepared using reprecipiation techniques that, like most H-type NFs, exhibited no PL quenching regardless of excitation intensity (see Supporting Information). The smaller PL quenching response observed in H-type NFs further demonstrates these morphologies more closely resemble those of thin films (*i.e.*, smaller aggregates with low intrachain order bordered by interpenetrating amorphous chains).

There is an additional possibility that fragmentation of NFs upon dilution and dispersion into polystyrene hosts can result in the presence of single P3HT molecules,[8] which may contribute to unwanted background signal modulation. However, single P3HT molecule PL intensities are much lower than NFs, and measurements of backgrounds showed no evidence of PL quenching. NF PL transients (insets in Figure 2b,c) recorded on longer time scales (~1−10 ms dwell times/channel) with a multichannel scaler show good photostability when subjected to pulsed excitation, unlike single molecules, which normally tend to flicker and degrade much faster. Longer time scale PL transients from anisole H-type NFs frequently exhibited small fluctuations between intermediate levels but usually not much larger than the shot noise, which probably originates from stochastic switching due to

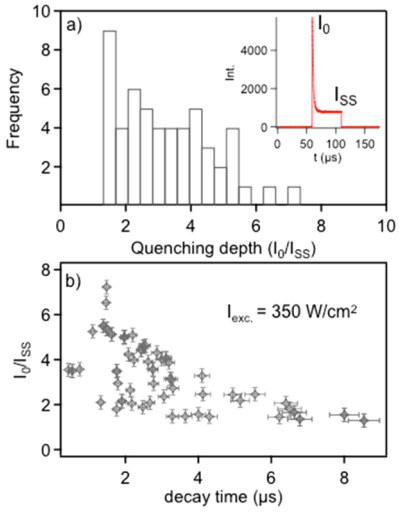

Figure 3. (a) Histogram of I_0/I_{SS} values of many J-type P3HT NF samples and (b) comparison of I_0/I_{SS} with decay times generated from single-exponential fits for a particular laser excitation intensity (I_{exc} = 350 W/cm^2).

energy transfer between distinct domains within the NF structure. Importantly, quenching depths and dynamics were dependent on excitation intensity (Figure 2b,c), revealing key insights into the mechanism(s) of PL quenching in P3HT NFs (*vide infra*).

We now focus on J-type P3HT NFs and classify their PL quenching ratios and decay time scales to identify the dominant quenching species and their possible formation mechanism(s). Representative distributions of I_0/I_{SS} values and decay times are shown in Figure 3a,b, respectively, within a particular sample (I_{exc} = 350 W/cm^2). Average I_0/I_{SS} values for J-type NFs are ~3.6 for excitation intensities of >250 W/cm^2. A single-exponential decay function of the empirical form

$$I(t) \propto I_0 \exp(-t/\tau) + I_{SS} \quad (1)$$

was fitted to excitation intensity-dependent MCA transients, and quenching time scales (I_{exc} = 350 W/cm^2) were compared to I_0/I_{SS} values (Figure 3b). Larger I_0/I_{SS} values (>2) correlate with faster quenching dynamics, a trend noted earlier in intensity-dependent PL quenching of single polymer molecules,[20] but decay time scales associated with smaller I_0/I_{SS} values (~1.5 or less) have a broader range (*i.e.*, ~1−10 μs). The variation of quenching dynamics and I_0/I_{SS} with excitation intensities indicates a bimolecular process,[35] probably involving multiple steps preceding PL quenching time scales observed here.

On the basis of previous photophysical studies of P3HT and related polythiophene systems, it is straightforward to arrive at two likely candidate PL quencher species in P3HT NFs, namely, polarons and triplet states. Polaronic species, such as free charges or loosely bound, uncorrelated polaron pairs, are often present in appreciable levels, but their optical cross sections are

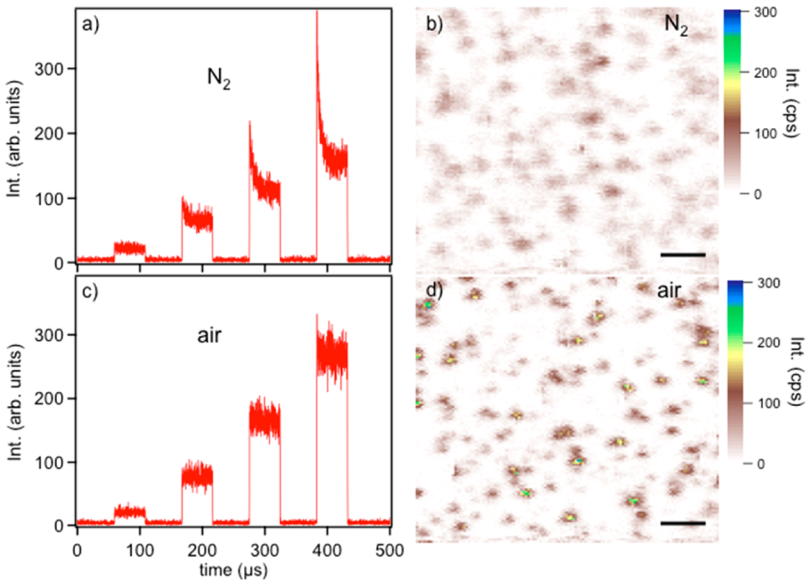

Figure 4. Representative single J-type NF intensity-dependent PL transients and images measured under N_2 (a, b) and air (c, d).

generally weak and spectral line shapes are broad and unresolved. As mentioned briefly in the introduction, the generation of polarons or polaron pairs in neat polymers has become an increasingly important topic for reconciling performance characteristics in optoelectronic devices,[11] but it is difficult to reliably control the yields of polaronic species in conventional thin-film structures due to morphological inhomogeneity. Interestingly, embedding single molecules in model unipolar OLED-type devices has demonstrated that polaron levels can be controlled with device bias, thus allowing detailed molecular-level studies of exciton–polaron interactions.[29]

Triplet excitons are relatively long-lived and can quench emissive singlets by energy transfer.[36] Triplets have received considerable attention for polymer solar cell applications since population of these low-energy states can be particularly detrimental because chromophores are effectively removed from photoexcitation cycling into allowed singlet states.[37] Strategies to either utilize or mitigate triplets have been pursued that have sought to take advantage of their longer lifetimes and, hence, larger diffusion lengths, although some studies suggest similar migration length scales as singlets.[36] The specific structural factors regulating triplet formation mechanisms and yields in polymers and related aggregates are still debated, but the prevailing consensus is that chromophore structural characteristics, such as intra- and interchain order, play an important role in determining triplet yields and dynamics.[36] Unfortunately, the subtle aspects of chain conformational and packing order are often masked in thin-film and solution spectroscopic studies from ensemble averaging effects. As demonstrated in Figures 2 and 3, these limitations can be circumvented in self-assembled NFs, especially for J-type NFs, owing to the ability to direct polymer conformation and packing.

Despite the promise of self-assembled NFs to resolve exciton–polaron interconversion and interactions, distinguishing either polarons or triplets as singlet-exciton quenchers in P3HT NF intensity-dependent transients can be a difficult task because they may coexist and interact over similar time scales. However, when triplet energies are >1 eV, the presence of oxygen quenches triplets by efficient energy transfer, thus sensitizing singlet oxygen, thereby providing a valuable diagnostic tool for revealing the presence of these states in NFs. We now perform single NF imaging and excitation intensity-dependent transient studies by regulating the atmosphere over NF solid dispersions. Samples for this study were processed without the aluminum overcoating and placed in a flow cell, where they were initially kept under a dry N_2 environment. Ambient air was then bled into the flow cell, and NF PL images and transients were recorded to help uncover the identity of the dominant quenching species in J-type NFs. Figure 4 shows representative J-type single NF spectra and PL images under N_2 (a, b) and exposed to air (c, d) using the same average laser power (~50 nW).

Unsealed samples recorded under dry N_2 environments show the typical efficient intensity-dependent PL quenching behavior albeit with somewhat lower signal-to-noise ratios because they lack the metal overcoating (Figure 4a). PL quenching behavior in single J-type NFs disappears or is strongly attenuated almost immediately after samples are exposed to air (I_0/I_{SS} ~1), consistent with previously published oxygen diffusion constants in P3HT.[38] Average PL

intensities initially display small, transient increases, which is discernible from comparison of the integrated intensities of transients before and after exposure to ambient air (Figure 4a,c), but then subsequently decrease from irreversible photodegradation processes. Excitation intensity-dependent transients were also recorded simultaneously with PL image acquisition by averaging over all particles in the image field-of-view that show similar behavior to single NFs in Figure 4a,c (see Supporting Information). The same experiments were performed on H-type NFs, and virtually no change in PL quenching behavior was observed upon exposure to air, demonstrating a much smaller amount of oxygen-sensitive quenchers formed (see Supporting Information).

The strong sensitivity of J-type NF PL quenching behavior to the presence of oxygen and lack of extended dark periods in corresponding PL transients indicate the dominant quenchers are triplet states. Previous reports of excitation intensity-dependent triplet quenching in single poly(3-octylthiophene) (P3OT) molecules showed similar behavior where average PL intensities increase substantially upon introduction of oxygen.[39] Schindler *et al*. performed PL imaging and transients on single ladder-type, poly(*para*-phenylene) molecules (MeLPPP) and were able to induce controlled bursts by introduction of air in the sample.[40] More recently, Steiner *et al*. used fluorescence correlation spectroscopy (FCS) to measure "on" and "off" times due to triplet blinking on single P3HT chains of varying molecular weight.[20] These authors found "on" times ranging from ~5 to 10 μs, which are comparable to PL quenching time scales reported here. Using the reported bimolecular rate constant of triplet quenching by oxygen in structurally similar P3OT ($k_Q = 1.4 \times 10^9$ M^{-1} s^{-1})[41] as an upper limit for P3HT aggregate triplets, triplet deactivation is expected to be very efficient in J-type NFs assuming high intrachain mobilities.

Further conformation of triplets as the dominant quenchers in P3HT NFs comes from detailed electron spin resonance and optically detected magnetic resonance studies of P3HT. Sperlich *et al*. observed both reversible and irreversible interactions with oxygen,[42] where the latter proceeds *via* triplet states. Reversible interactions with oxygen were shown to involve singlet excitons that usually manifest as long "off" times in PL transients of single polymer molecules from charge transfer complex formation with oxygen.[24] The introduction of ambient air into unsealed J-type NF samples, along with larger peak intensities from pulsed excitation, accelerates photodegradation and loss of PL signal due to the highly electrophilic character of singlet oxygen generated by triplet sensitization, which is not characteristic of a reversible charge transfer complex interaction.[42] Although these types of interactions with oxygen are possible and commonly observed in single-molecule spectroscopy of polymers, they are probably masked in our data owing to the multichromophoric nature of NFs.

Mechanisms of Triplet Formation in J-Aggregate P3HT Nanofibers. Despite apparent efficient triplet generation and quenching in J-type P3HT NFs, it is noteworthy that previous transient absorption spectroscopic studies of regioregular P3HT thin films instead showed preferential polaron generation.[12,13] This situation changes dramatically in P3HT solutions, where appreciable triplet populations were reported in P3HT chains with significant dynamic conformational disorder.[43] From comparison of intensity-dependent PL transient trends from H- and J-type NFs, the stark contrast in apparent triplet−polaron branching ratios in these P3HT forms can most readily be traced to differences in chain conformational and packing order. Similar dependences were reported earlier from photophysical studies of amorphous (glassy) and crystalline (β-phase) poly(9,9-di-*n*-octylfluorenyl-2,7-diyl) thin films, which show much lower triplet populations for the planar β-phase due to efficient polaron generation.[44]

The expected low triplet yields observed in polymer thin-film aggregates raise questions regarding the mechanisms in effect for efficient triplet generation in J-type NFs. It is first important to point out that the structural qualities of these aggregates are significantly different from those typically encountered in conventional polymer thin films and solution phase conformations. We propose that the unusually high intrachain order and packing integrity of these aggregates play key roles in determining the photophysical outcomes resulting in triplet formation, and we now consider several candidate triplet mechanisms known to be operative in conjugated organic molecules, namely, (i) singlet fission; (ii) intersystem crossing (ISC); and (iii) nongeminate polaron recombination to triplets.

Singlet exciton fission has received a great deal of attention lately for its potential to increase yields of photogenerated charge carriers in solar cells.[31] This process involves conversion of optically allowed singlet states into two spin-forbidden triplets on neighboring chromophores promptly following photoexcitation.[45] However, singlet excitation energies must be at least 2 times larger than the lowest energy triplet ($E_{S1} \geq 2E_{T1}$), making singlet fission more efficient in chromophores with large exchange energies and S_1-T_1 energy gaps (ΔE_{S-T}).[45] Although singlet fission was shown to generate triplets on ultrafast time scales in P3HT solutions,[13] we rule it out as a likely mechanism of PL quenching by triplets on microsecond time scales (Figures 2 and 3) since high intrachain order in J-type NFs and persistent, delocalized intrachain exciton character over its entire lifetime should result in lower exchange energies and ΔE_{S-T}.[46] Moreover, the excitation energy used to excite PL (568 nm, 2.18 eV) is not far above the optical gap, which would further reduce singlet fission efficiency.

Excited-state spin crossover on conjugated organic chromophores is more commonly reported on longer time scales (>1 ns), which typically corresponds to ISC events requiring sufficient spin−orbit coupling.[46] Bredas and co-workers calculated the ISC rate constant for planar oligothiophenes (idealized C_{2h} point group symmetry) and predicted very small triplet yields since spin−orbit mixing of the lowest energy excited singlet (^1B_u) and triplet (^3B_u) is possible only for the *z*-component (A_g) of the spin−orbit coupling.[47] This mechanism requires an out-of-plane backbone distortion in order to achieve nonzero spin−orbit S_1−T_1 mixing, which is better realized in solution-like, P3HT chain conformations with dynamic conformational disorder.[47] The stringent symmetry factors imposed by relatively planar P3HT chains in J-type NFs could possibly be circumvented by the expected lower exchange energies mentioned above. Consequently, smaller ΔE_{S-T} values could result in an increase of the ISC rate constant, although spin−orbit mixing of singlets and triplets is small.[48] Previous studies of exchange energies in a variety of polymers show a near constant value (~0.7 eV) in addition to similar ΔE_{S-T} values.[36] It is important to stress these studies were performed in solution and solid thin films with nonfractionated samples, which could potentially mask contributions from minority chains with high intrachain order common to J-type NFs. A comparison of heavy atom effects in π-stacked aggregates with high conformational order could perhaps better assess ISC yields, but such materials are not presently available for this study.[49]

Another intriguing ISC pathway involves coupling S_1 to higher energy triplet states (T_n) in closer energetic proximity to S_1 with favorable symmetry followed by rapid internal conversion to the lowest energy triplet, T_1. This multistep process essentially mimics lowering exchange energies, but triplet−triplet absorption spectra of P3HT and related polymer systems show no evidence of higher energy triplet states in the energetic vicinity of the S_1 state.[36] At this stage, it is not possible to definitively rule out ISC as a viable mechanism for efficient generation of triplets in J-type NFs. Nonetheless, the structural and symmetry factors responsible for the dominant J-aggregate exciton coupling conflict with established literature trends relating structural factors and ΔE_{S-T} indicating that ISC should not be efficient.

Similar to previous studies of autoionization processes in regioregular P3HT thin films, Martin *et al.* measured ultrafast transient absorption spectra for H- and J-type P3HT NF dispersions and found no distinct triplet signatures appearing on time scales ranging from ~200 fs up to ~1 ns.[34] On the other hand, delocalized polarons (DP) and intrachain polaron pairs (PP)[50] were reported with significantly longer lifetimes in J-type NFs compared to their H-type counterparts.[34] At early time scales (<200 fs) the PP:DP change in optical density (ΔOD) signal ratio was 10:1 for J-type NFs compared to a value of 1.5:1 found in anisole-assembled H-type NFs.[34] This result highlighted the stark contrast of intrachain order in both NF types, which serves to delocalize excitons and increase electron−electron correlation lengths. Although PP relaxation times were similar for both NFs,[31] DP species showed much slower relaxation dynamics (τ > 2 ns) in J-type NFs since they are more sensitive to interchain coupling,[34] which is virtually absent in these aggregates.

The long-lived nature of uncorrelated intrachain DP species potentially sets the stage for nongeminate recombination at later times when these populations become significantly larger than earlier time scales probed by ultrafast spectroscopy. According to simple spin statistics, recombination of uncorrelated polarons to triplet *vs* singlet states should have a 3:1 branching ratio, respectively. Similar triplet generation mechanisms were proposed in *para*-hexaphenyl[51] and poly(phenylene−vinylene),[15] although the ordering and size of these chromophores are probably lower than in J-type P3HT NFs. Because PP and DP species tend to recombine geminately on much faster time scales in H-type NFs due to the more localized character and larger interchain coupling, triplet recombination yields in these aggregates are expected to be small, resulting in much lower or no PL quenching on microsecond time scales, as shown in Figure 2b. This result is also consistent with previously reported low triplet yields in P3HT thin films owing to the morphological similarities between films and H-type NFs.

It is also noteworthy that several groups have demonstrated that polaron recombination does not always follow simple spin statistics. For example, increasing conjugation lengths (*e.g.*, regioregular aggregated P3HT *vs* regiorandom amorphous P3HT) tends to favor increased recombination to singlets, which is consistent with smaller ΔE_{S-T}.[52,53] While our present results do not enable us to quantitatively estimate the triplet populations from PP/DP recombination, the longer triplet lifetime and expected diffusion lengths still result in effective PL quenching of singlet excitons, even at lower populations than predicted from spin recombination statistics. On the basis of these considerations, we attribute triplet formation on >1 ns time scales in J-type NFs largely to nongeminate recombination of polarons generated on earlier time scales.

Regardless of the specific mechanism of formation, the spin-forbidden, nonradiative relaxation back to the ground electronic state (S_0) of triplets occurs by reverse ISC and should be similar to values reported from other P3HT forms (*i.e.*, thin films, nanoparticles, and single molecules). We use a sequence of two excitation pulses delayed with respect to each other that reveal triplet quencher relaxation time scales *via* reverse ISC and

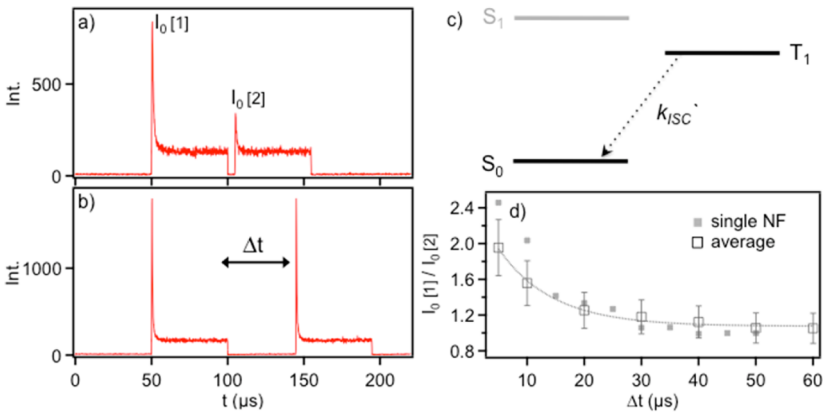

Figure 5. (a, b) Variable pulse time gap single NF PL experiment on sealed NF samples. Pulses of the same intensity and duration are delayed on time scales of ~5−100 μs. (c) Reverse ISC process probed by the variable time delay pulsed excitation PL experiment. (d) Comparison of initial intensities (I_0) for each pulse and their respective time delays (Δt) for a single NF (solid squares) and ensemble averaged NFs acquired from many individual particles for each time delay.

compare the results to established literature trends. A steady-state triplet population is generated by the first PL excitation pulse that subsequently decays to S_0 in the dark by reverse ISC once the pulse shuts off. By delaying the second pulse to excite the NF particle within the expected triplet lifetime, the ratio of initial intensities generated from both pulses ($I_0[1]/I_0[2]$) with respect to the pulse time delay (Δt) exposes the presence of unrelaxed triplets apparent from quenching of $I_0[2]$ levels.

Figure 5 shows representative J-type NF spectra generated in samples with aluminum overcoatings at short (a, 5 μs) and long (b, 40 μs) delays. $I_0[1]/I_0[2]$ values are plotted with their respective delay time, Δt, for a single NF and average over ~30 particles collected over various delay times. A single-exponential fit to these curves produces an average time constant of ~9 μs, which we assign to reverse ISC back to the ground S_0 state (Figure 5d). This value is within a factor of 2 of reverse ISC rate constant estimates determined from single P3OT molecules (k_{ISC}' ~16 μs) using a coupled photodynamic model in addition to average "off" times of 18 μs determined from FCS measurements of single P3HT molecules.[20] The faster triplet relaxation time scales found in NFs are consistent with observations from previous studies of size-dependent energy transfer and polaron dynamics in conjugated polymer nanostructures.[18] While increasing Δt in these experiments does increase peak excitation intensities, taking the ratio of I_0 values from both pulses removes this dependence, allowing for comparison of triplet relaxation between various pulse delay times. Moreover, quenching dynamics time scales were always within the range reported earlier in Figure 3. PL rise times for both pulses were also identical and showed no variation with the delay time of the second pulse (see Supporting Information).

CONCLUSIONS

We have shown that high intrachain order in J-type P3HT NFs facilitates delocalization of excitons, leading to the eventual formation of triplets from nongeminate recombination of delocalized polaron species. These mobile triplets interact with emissive singlet excitons and lead to efficient PL quenching on microsecond time scales. The identity of triplets as the dominant quenching species was confirmed from the strong sensitivity of PL modulation depths, I_0/I_{SS}, to the presence of oxygen. By comparing excitation intensity-dependent PL quenching responses from J-type and less-ordered H-type NFs, previously reported low triplet yields encountered in thin films can be explained in terms of P3HT chain ordering within the aggregate. Namely, lower intrachain order in H-type P3HT aggregates localizes excitons and polarons, making nongeminate polaron recombination to triplets inefficient due to the dominance of faster geminate recombination processes. Overall, our results demonstrate the potential of self-assembled polymer nanostructures to understand and, ultimately, control the photophysics responsible for populating various spin states over a wide range of time scales. We further propose that reliable control of polymer intrachain order within coupled, multichromophore systems might eventually prove useful for manipulating spin populations and transporting these species over larger distance scales than what is currently possible in conventional polymer functional forms.

METHODS

NFs are assembled using regioregular P3HT (Plextronics; M_n = 65 kDa, PDI = 1.3), then dispersed in inert hosts and probed individually by intensity-modulated single-nanoparticle PL spectroscopy and imaging. The complete description of the fabrication as well as structural and photophysical characterization of

these NFs can be found in refs 8 and 34. Briefly, J-type NFs were formed by controlled self-assembly for >24 h in toluene solutions, resulting in well-ordered π-stacked structures with high molecular weight fractionation and intrachain order.[8] Mixed H-type NFs formed rapidly in anisole are composed of kinetically trapped conformations and aggregate packing arrangements, giving rise to polymorphic domains within the NF due to the highly inclusive manner of assembly (*i.e.*, no molecular weight fractionation).[34]

Following formation and subsequent purification steps, both NF types were dispersed in an inert host matrix (polystyrene GPC standard, M_n = 70 kDa) and spin-coated onto rigorously cleaned glass coverslips inside a nitrogen-circulating glovebox. To prevent oxygen- and water-induced photochemistry and photobleaching, samples were placed under high vacuum for ~60 min ($<10^{-6}$ mbar), and aluminum was deposited by thermal evaporation on top of the NF solid dispersions (~150−200 nm). Excitation intensity-dependent single-nanoparticle spectroscopy and imaging was then used to study nano- to microsecond time-resolved PL of isolated P3HT NFs (see Figure 1e). The unpolarized 568 nm output of a CW krypton ion laser (Melles-Griot) serves as the excitation source corresponding to the absorption maximum of P3HT aggregates (as indicated by arrows in Figures 1c,d). The laser was modulated using an acoustic optical modulator (Intra-action) controlled by a function generator to produce stairstep, on−off pulse sequences of varying time duration and intensity. Modulated excitation light was next focused to a diffraction-limited spot in a home-built confocal scanning microscope (NA = 1.4, 100×) equipped with a nanopositioning stage (Madcity). PL from individual P3HT NFs was detected using a single photon counting avalanche photodiode (APD, PerkinElmer SPCM-AQR-15), and a long-pass edge filter (Semrock) removed scattered excitation light before the detector. Excitation intensity-dependent transients were recorded using a multichannel analyzer (MCA-3, Fast Comtec) by synchronously averaging many (>10 000) excitation pulse cycles. To further ensure suppression of photodegradation, samples were placed in a dry nitrogen flow cell on the microscope. Simultaneous integrated PL intensity transients were also measured over longer dwell times (~1−10 ms) to monitor photo-oxidation and photobleaching effects in sealed samples under nitrogen, which were minor (*i.e.*, <10% of NFs showed appreciable degradation over the course of the experiment, ~3−5 min). Areal densities of NF PL images varied linearly with concentration, indicating that particles were not agglomerating prior to deposition (see Supporting Information).

Conflict of Interest: The authors declare no competing financial interest.

Supporting Information Available: NF concentration-dependent PL images, effect of pulse cycle period on intensity-dependent PL quenching, averaged areal integrated intensity of H- and J-type NFs, effect of intensity-modulated pulsed excitation on bulk P3HT thin films, rise time of NF PL intensities with varying pulse time delay. This material is available free of charge *via* the Internet at http://pubs.acs.org.

Acknowledgment. We acknowledge valuable discussions with Prof. Martin Kirk, and J.K.G. acknowledges financial support from the National Science Foundation (CHE-0955242 and IIA-1301346).

REFERENCES AND NOTES

1. Schwartz, B. J. Conjugated Polymers as Molecular Materials: How Chain Conformation and Film Morphology Influence Energy Transfer and Interchain Interactions. *Annu. Rev. Phys. Chem.* **2003**, *54*, 141–172.
2. Brinkmann, M. Structure and Morphology Control in Thin Films of Regioregular Poly(3-hexylthiophene). *J. Polym. Sci., Part B* **2011**, *49*, 1218–1233.
3. Sirringhaus, H.; Brown, P. J.; Friend, R. H.; Nielsen, M. M.; Bechgaard, K.; Langeveld-Voss, B. M. W.; Spiering, A. J. H.; Janssen, R. A. J.; Meijer, E. W.; Herwig, P.; *et al*. Two-Dimensional Charge Transport in Self-Organized, High-Mobility Conjugated Polymers. *Nature* **1999**, *401*, 685–688.
4. Osterbacka, R.; An, C. P.; Jiang, X. M.; Vardeny, Z. V. Two-Dimensional Electronic Excitations in Self-Assembled Conjugated Polymer Nanocrystals. *Science* **2000**, *287*, 839–842.
5. Spano, F. C. The Spectral Signatures of Frenkel Polarons in H- and J-Aggregates. *Acc. Chem. Res.* **2010**, *43*, 429–439.
6. Yamagata, H.; Spano, F. C. Interplay between Intrachain and Interchain Interactions in Semiconducting Polymer Assemblies: The HJ-Aggregate Model. *J. Chem. Phys.* **2012**, *136*, 184901/1–184901/14.
7. Clark, J.; Silva, C.; Friend, R. H.; Spano, F. C. Role of Intermolecular Coupling in the Photophysics of Disordered Organic Semiconductors: Aggregate Emission in Regioregular Polythiophene. *Phys. Rev. Lett.* **2007**, *98*, 206406/1–206406/4.
8. Niles, E. T.; Roehling, J. D.; Yamagata, H.; Wise, A. J.; Spano, F. C.; Moulé, A. J.; Grey, J. K. J-Aggregate Behavior in Poly(3-hexylthiophene) Nanofibers. *J. Phys. Chem. Lett.* **2012**, *3*, 259–263.
9. Roehling, J. D.; Arslan, I.; Moule, A. J. Controlling Microstructure in Poly(3-hexylthiophene) Nanofibers. *J. Mater. Chem. C* **2012**, *22*, 2498–2506.
10. Paquin, F.; Latini, G.; Sakowicz, M.; Karsenti, P.-L.; Wang, L.; Beljonne, D.; Stingelin, N.; Silva, C. Charge Separation in Semicrystalline Polymeric Semiconductors by Photoexcitation: Is the Mechanism Intrinsic or Extrinsic? *Phys. Rev. Lett.* **2011**, *106*, 197401/1–197401/4.
11. Reid, O. G.; Pensack, R. D.; Song, Y.; Scholes, G. D. Rumbles, G., Charge Photogeneration in Neat Conjugated Polymers. *Chem. Mater.* **2014**, *26*, 561–575.
12. Paquin, F.; Yamagata, H.; Hestand, N. J.; Sakowicz, M.; Berube, N.; Cote, M.; Reynolds, L. X.; Haque, S. A.; Stingelin, N.; Spano, F. C.; Silva, C. Two-Dimensional Spatial Coherence of Excitons in Semicrystalline Polymeric Semiconductors: Effect of Molecular Weight. *Phys. Rev. B* **2013**, *88*, 155202/1–155202/14.
13. Guo, J.; Ohkita, H.; Benten, H.; Ito, S. Near-IR Femtosecond Transient Absorption Spectroscopy of Ultrafast Polaron and Triplet Exciton Formation in Polythiophene Films with Different Regioregularities. *J. Am. Chem. Soc.* **2009**, *131*, 16869–16880.
14. Tapping, P. C.; Kee, T. W. Optical Pumping of Poly(3-hexylthiophene) Singlet Excitons Induces Charge Carrier Generation. *J. Phys. Chem. Lett.* **2014**, *5*, 1040–1047.
15. Dyakonov, V.; Frankevich, E. On the Role Played by Polaron Pairs in Photophysical Processes in Semiconducting Polymers. *Chem. Phys.* **1998**, *227*, 203–217.
16. Hu, D. H.; Yu, J.; Wong, K.; Bagchi, B.; Rossky, P. J.; Barbara, P. F. Collapse of Stiff Conjugated Polymers with Chemical Defects into Ordered, Cylindrical Conformations. *Nature* **2000**, *405*, 1030–1033.
17. Yu, J.; Hu, D.; Barbara, P. F. Unmasking Electronic Energy Transfer of Conjugated Polymers by Suppression of O_2 Quenching. *Science* **2000**, *289*, 1327–1330.
18. Grey, J. K.; Kim, D. Y.; Norris, B. C.; Miller, W. L.; Barbara, P. F. Size Dependent Spectroscopic Properties of Conjugated Polymer Nanoparticles. *J. Phys. Chem. B* **2006**, *110*, 25568–25572.
19. Huser, T.; Yan, M.; Rothberg, L. J. Single Chain Spectroscopy of Conformational Dependence of Conjugated Polymer Photophysics. *Proc. Natl. Acad. Sci. U.S.A.* **2000**, *97*, 11187–11191.
20. Steiner, F.; Vogelsang, J.; Lupton, J. M. Singlet-Triplet Annihilation Limits Exciton Yield in Poly(3-hexylthiophene). *Phys. Rev. Lett.* **2014**, *112*, 137402/1–137402/5.
21. Kim, D. Y.; Grey, J. K.; Barbara, P. F. A Detailed Single Molecule Spectroscopy Study of the Vibronic States and Energy Transfer Pathways of the Conjugated Polymer MEH-PPV. *Synth. Met.* **2006**, *156*, 336–345.
22. Bolinger, J. C.; Traub, M. C.; Brazard, J.; Adachi, T.; Barbara, P. F.; Vanden Bout, D. A. Conformation and Energy Transfer in Single Conjugated Polymers. *Acc. Chem. Res.* **2012**, *45*, 1992–2001.

23. Gesquiere, A. J.; Park, S. J.; Barbara, P. F. F-V/SMS: A New Technique for Studying the Structure and Dynamics of Single Molecules and Nanoparticles. *J. Phys. Chem. B* **2004**, *108*, 10301–10308.
24. Barbara, P. F.; Gesquiere, A. J.; Park, S.-J.; Lee, Y. J. Single-Molecule Spectroscopy of Conjugated Polymers. *Acc. Chem. Res.* **2005**, *38*, 602–610.
25. Bolinger, J. C.; Traub, M. C.; Adachi, T.; Barbara, P. F. Ultralong-Range Polaron-Induced Quenching of Excitons in Isolated Conjugated Polymers. *Science* **2011**, *331*, 565–567.
26. Vosch, T.; Hofkens, J.; Cotlet, M.; Kohn, F.; Fujiwara, H.; Gronheid, R.; Van Der Biest, K.; Weil, T.; Herrmann, A.; Mullen, K.; Mukamel, S.; Van der Auweraer, M.; De Schryver, F. C. Influence of Structural and Rotational Isomerism on the Triplet Blinking of Individual Dendrimer Molecules. *Angew. Chem., Int. Ed.* **2001**, *40*, 4643–4647.
27. Gesquiere, A. J.; Lee, Y. J.; Yu, J.; Barbara, P. F. Single Molecule Modulation Spectroscopy of Conjugated Polymers. *J. Phys. Chem. B* **2005**, *109*, 12366–12371.
28. Yamagata, H.; Pochas, C. M.; Spano, F. C. Designing J- and H-Aggregates through Wave Function Overlap Engineering: Applications to Poly(3-hexylthiophene). *J. Phys. Chem. B* **2012**, *116*, 14494–14503.
29. Gesquiere, A. J.; Park, S.-J.; Barbara, P. F. Hole-Induced Quenching of Triplet and Singlet Excitons in Conjugated Polymers. *J. Am. Chem. Soc.* **2005**, *127*, 9556–9560.
30. Wohlgenannt, M.; Vardeny, Z. V.; Frolov, S. V.; Kloc, C.; Batlogg, B. Long-Lived Photoexcitations in α-Hexathiophene Single Crystals. *Synth. Met.* **2001**, *116*, 181–184.
31. Barford, W. Exciton Transfer Integrals between Polymer Chains. *J. Chem. Phys.* **2007**, *126*, 134905/1–134905/6.
32. Baghgar, M.; Labastide, J.; Bokel, F.; Dujovne, I.; McKenna, A.; Barnes, A. M.; Pentzer, E.; Emrick, T.; Hayward, R.; Barnes, M. D. Probing Inter- and Intrachain Exciton Coupling in Isolated Poly(3-hexylthiophene) Nanofibers: Effect of Solvation and Regioregularity. *J. Phys. Chem. Lett.* **2012**, *3*, 1674–1679.
33. Baghgar, M.; Labastide, J. A.; Bokel, F.; Hayward, R. C.; Barnes, M. D. Effect of Polymer Chain Folding on the Transition from H- to J-Aggregate Behavior in P3HT Nanofibers. *J. Phys. Chem. C* **2014**, *118*, 2229–2235.
34. Martin, T. P.; Wise, A. J.; Busby, E.; Gao, J.; Roehling, J. D.; Ford, M. J.; Larsen, D. S.; Moule, A. J.; Grey, J. K. Packing Dependent Electronic Coupling in Single Poly(3-hexylthiophene) H- and J-Aggregate Nanofibers. *J. Phys. Chem. B* **2013**, *117*, 4478–4487.
35. Yu, J.; Lammi, R.; Gesquiere, A. J.; Barbara, P. F. Singlet-Triplet and Triplet-Triplet Interactions in Conjugated Polymer Single Molecules. *J. Phys. Chem. B* **2005**, *109*, 10025–10034.
36. Koehler, A.; Baessler, H. Triplet States in Organic Semiconductors. *Mater. Sci. Eng.* **2009**, *R66*, 71–109.
37. Clarke, T. M.; Durrant, J. R. Charge Photogeneration in Organic Solar Cells. *Chem. Rev.* **2010**, *110*, 6736−6767.
38. Abdou, M. S. A.; Orfino, F. P.; Son, Y.; Holdcroft, S. Interaction of Oxygen with Conjugated Polymers: Charge Transfer Complex Formation with Poly(3-alkylthiophenes). *J. Am. Chem. Soc.* **1997**, *119*, 4518–4524.
39. Palacios, R. E.; Barbara, P. F. Single Molecule Spectroscopy of Poly 3-octyl-thiophene (P3OT). *J. Fluoresc.* **2007**, *17*, 749–757.
40. Schindler, F.; Lupton, J. M.; Feldmann, J.; Scherf, U. Controlled Fluorescence Bursts from Conjugated Polymers Induced by Triplet Quenching. *Adv. Mater.* **2004**, *16*, 653–657.
41. Burrows, H. D.; de Melo, J. S.; Serpa, C.; Arnaut, L. G.; Miguel, M. D.; Monkman, A. P.; Hamblett, I.; Navaratnam, S. Triplet State Dynamics on Isolated Conjugated Polymer Chains. *Chem. Phys.* **2002**, *285*, 3–11.
42. Sperlich, A.; Kraus, H.; Deibel, C.; Blok, H.; Schmidt, J.; Dyakonov, V. Reversible and Irreversible Interactions of Poly(3-hexylthiophene) with Oxygen Studied by Spin-Sensitive Methods. *J. Phys. Chem. B* **2011**, *115*, 13513–13518.
43. Cook, S.; Furube, A.; Katoh, R. Analysis of the Excited States of Regioregular Polythiophene P3HT. *Energy Environ. Sci.* **2008**, *1*, 294–299.
44. Hayer, A.; Khan, A. L. T.; Friend, R. H.; Kohler, A. Morphology Dependence of the Triplet Excited State Formation and Absorption in Polyfluorene. *Phys. Rev. B* **2005**, *71*, 241302/1–241302/4.
45. Smith, M. B.; Michl, J. Singlet Fission. *Chem. Rev.* **2010**, *110*, 6891–6936.
46. Monkman, A.; Burrows, H. D. Backbone Planarity Effects on Triplet Energies and Electron-Electron Correlation in Luminescent Conjugated Polymers. *Synth. Met.* **2004**, *141*, 81–86.
47. Beljonne, D.; Shuai, Z.; Pourtois, G.; Bredas, J. L. Spin-Orbit Coupling and Intersystem Crossing in Conjugated Polymers: A Configuration Interaction Description. *J. Phys. Chem. A* **2001**, *105*, 3899–3907.
48. Turro, N. J. *Modern Molecular Photochemistry*; University Science Books: Mill Valley, CA, 1978.
49. Pensack, R. D.; Song, Y.; McCormick, T. M.; Jahnke, A. A.; Hollinger, J.; Seferos, D. S.; Scholes, G. D. Evidence for the Rapid Conversion of Primary Photoexcitations to Triplet States in Seleno- and Telluro- Analogues of Poly-(3-hexylthiophene). *J. Phys. Chem. B* **2014**, *118*, 2589–2597.
50. Ruseckas, A.; Theander, M.; Andersson, M. R.; Svensson, M.; Prato, M.; Inganas, O.; Sundstrom, V. Ultrafast Photogeneration of Inter-chain Charge Pairs in Polythiophene Films. *Chem. Phys. Lett.* **2000**, *322*, 136–142.
51. Zenz, C.; Cerullo, G.; Lanzani, G.; Graupner, W.; Meghdadi, F.; Leising, G.; De Silvestri, S. Ultrafast Photogeneration Mechanisms of Triplet States in para-Hexaphenyl. *Phys. Rev. B* **1999**, *59*, 14336–14341.
52. Wohlgenannt, M.; Jiang, X. M.; Yang, C.; Korovyanko, O. J.; Vardeny, Z. V. Spin-Dependent Polaron Pair Recombination in π-Conjugated Polymers: Enhanced Singlet Exciton Densities. *Synth. Met.* **2003**, *139*, 921–924.
53. Wohlgenannt, M.; Jiang, X. M.; Vardeny, Z. V.; Janssen, R. A. J. Conjugation-Length Dependence of Spin-Dependent Exciton Formation Rates in π-Conjugated Oligomers and Polymers. *Phys. Rev. Lett.* **2002**, *88*, 197401/1–197401/4.